31st Annual International Conference of the IEEE EMBS
Minneapolis, Minnesota, USA, September 2-6, 2009

A CCD Based Approach to Collimated Photon Counting Imaging for Micro-SPECT/CT

Diane R. Eaker, Bogdan Dzyubak, Steven M. Jorgensen, Erik L. Ritman

***Abstract*—Analog summation methods of x-ray imaging have nonlinearity in signal readout and dynamic range limitations. To minimize these limitations, a photon counting CCD-based gamma camera imaging system has been developed and evaluated.**

I. Introduction

In biological applications, a 1% noise to signal ratio is desirable and the imaging process must be completed within seconds or perhaps minutes at most. Hence, 10,000 photons/second/voxel are desirable. As we expect to use of the order of 360 angles of view during a CT scan, we need to record 10,000/360 photon/second/detector pixel of the x-ray detector, i.e., ~30 photons/pixel/second. Hence, if a CCD is read out at 100 frames/second then each detector pixel, on average, would record 0.3 photons, or every third pixel would record 1 photon. As the small signals generated by a single photon can be obscured by electronic noise in the CCD camera system, the x-ray image signal needs to be amplified with an image intensifier, such as a Micro Channel Plate Image Intensifier (MCPII) in our case. A secondary problem is that of photon superposition and discriminating between photons of different energy by virtue of their CCD image brightness value (which might look like superimposed lower energy photons).

II. METHODS

A. System Characterization

Fig. 1 is a schematic of the experimental set up. Distance L was selected so that the brachytherapy seeds containing 3.5 mCi ^{125}I or 1.05 mCi ^{103}Pd, exposed the x-ray-to-light scintillator with equal photon flux. The ^{125}I emits photons with predominately 27 keV and ^{103}Pd emits photons predominately 20 keV, (Fig. 2).

Manuscript received June 19, 2009. This work was supported in part by the NIH under Grant EB000305.

D. R. Eaker is with the Department of Physiology and Biomedical Engineering, Mayo Clinic College of Medicine of Rochester, MN 55905 USA.(e-mail: eaker.diane@mayo.edu)

B. Dzyubak is with the Department of Biomedical Engineering, University of Wisconsin-Madison, Madison, WI 53706 USA (e-mail: dzyubak@wisc.edu).

S. M. Jorgensen is with the Department of Physiology and Biomedical Engineering, Mayo Clinic College of Medicine of Rochester, MN 55905 USA (e-mail: smjorgensen@mayo.edu)

E. L. Ritman is with the Department of Physiology and Biomedical Engineering, Mayo Clinic College of Medicine of Rochester, MN 55905 USA. (corresponding author phone: 507-255-1939 fax: 507-255-1935; e-mail: elran@mayo.edu).

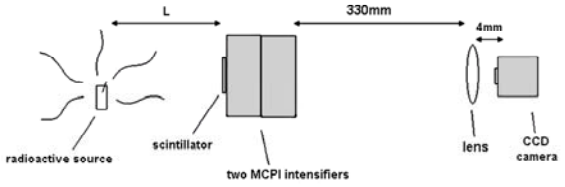

Fig. 1. Schematic of the system used to evaluate the photon counting and energy discriminating characteristics of the imaging system.

The x-ray detection system consists of a 31x32x0.15mm columnar CsI(Tl) scintillator with 70% detection efficiency at 25 KeV, a pair of oil-coupled MCPII (75mm diameter, 18 lp/mm, 9% Q efficiency at 540 nm) each with luminous gain up to15,000, a lens configured for 8x demagnification coupling the intensifier output to a CCD image array, which is operated at 100 frames per second readout rate with 640x480 $(7.4\mu m)^2$ pixels. It was operated in a progressive scan read out mode with 8 bit gray-scale. At the 540nm light output of the MCPII, the quantum efficiency of the CCD was 55%.

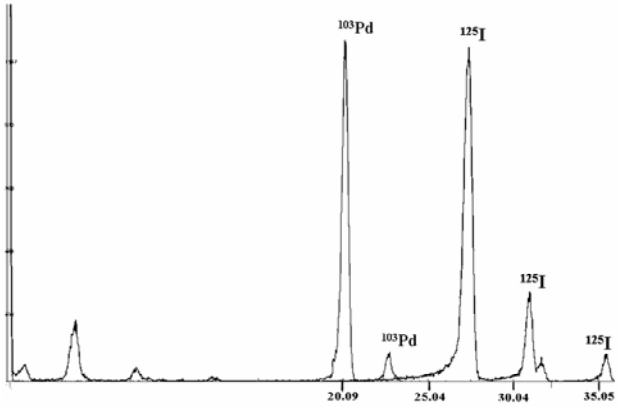

Fig. 2. Gamma ray spectra for ^{103}Pd and ^{125}I normalized so that the highest emission peaks of each are approximately equal in amplitude. These isotopes were chosen to establish the energy discrimination capability of the imaging system.

With the ^{103}Pd seed L = 127mm, ^{125}I seed L = 233mm, the

With the ^{103}Pd and L = 127mm, ^{125}I seed = 233mm. The expected photon count at the input of the detector assembly is:

$$(A*C*3.7x10^7 dps*E)/(4\pi*L^2*100 \text{ frames/sec}) \quad (1)$$

Where: A = area of scintillator (mm^2)
C = seed activity (mCi)
E = scintillator efficiency

Based on (1), the ^{125}I should generate 937 photons/frame and the ^{103}Pd 946 photons/frame.

To identify the scintillation caused by each photon, a threshold operation was applied to the CCD image so to eliminate the image noise (Fig. 3). A binary image was then generated, where black (0) is the background and white (1) is the "image feature" of interest. This process was automated by using a Matlab function [1] called "bwlabel" followed by a count of the resulting objects. An image feature was defined as a white pixel that touches another white pixel on a side or corner, i.e., single pixel signal is assumed to be noise other than a photon. The binary image was multiplied by the original grayscale image and the grayscales of each of the pixels in each of the separate features (i.e., a 'blob') were summed to provide the brightness of a 'blob'.

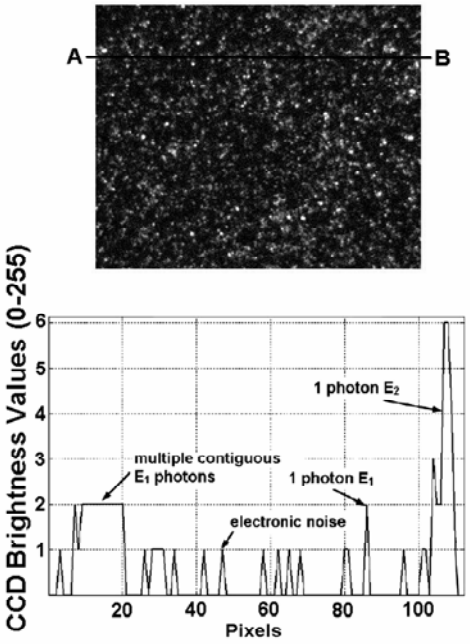

Fig. 3. Top Panel: Single CCD array frame (1/100 second). The fainter bright spots are noise due to the image intensifier and the CCD electronics. The larger cluster sizes are due to contiguous and/or overlapping photons arriving within the same CCD integration period. Bottom Panel: the intensity profile along part of the line A – B in the left panel. The "area" under the multiple E_1 photons aggregate could be equal to the area under one E_2 photon.

The size of a 'blob' due to a single photon is greater than one CCD pixel because of the ′blurring′ caused by the thickness of the CsI crystal, image intensifiers, and the coupling optics. In all cases the sum of all pixel grayscale values in the 'blob' should remain equal for all photons of the same energy and should increase linearly with increasing photon energy. Because the photons distribute randomly over the CCD array, the chance of photons being contiguous or superimposed follows a power law relationship – which is a straight line when plotted as a log/log relationship of frequency to total brightness of each 'blob' [2] as illustrated schematically in Fig. 4. The area under this curve should be equal to the number of photons multiplied by the total "brightness" generated by one photon. Hence, the area under this frequency/brightness curve, divided by the total number of photons expected to be captured in the image (1), should equal the brightness of a single photon. A grayscale threshold (T) is adjusted until the photon count so estimated equals the number of predicted photon hits.

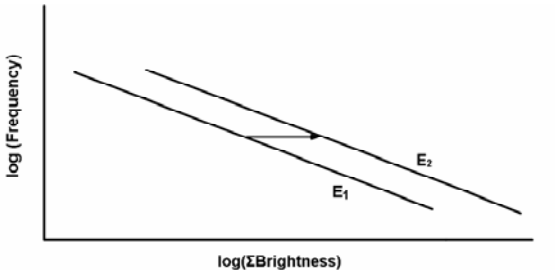

Fig. 4. Frequency histogram of aggregate (Σbrightness) relationship. Photon energy of photons E_1 < energy of photons E_2. The relationship shifts to the right with increased photon energy. This shift should be proportional to E_2-E_1).

B. Imaging System Performance

The system depicted in Fig. 1 was also operated with a parallel polycapillary optic [3], [4] placed between the brachytherapy seed and the CsI(Tl) x-ray to light converting fiber optic plate. This optic, which functions as an angular filter, was 25mm in diameter and 25mm thick and made up of 25 μm diameter hollow boron glass capillaries. An x-ray photon entering this capillary is transported to the other end of the capillary by virtue of total internal reflection. The acceptance angle of each capillary is such that 95% of photons are captured within 1.6 milli-radian). The ^{125}I brachytherapy seed contains four 0.7mm diameter spheres coated with ^{125}I. They are enclosed in a metal casing.

III. RESULTS

A. System Characteristics

As illustrated in Fig. 5, the differences between ^{125}I and ^{103}Pd frequency histograms were attributed to the different energy of the photons emitted by the two nuclides.

With this approach, the ^{125}I photon was computed to have an individual photon brightness of 7.77 brightness units/'blob' and the ^{103}Pd has a total brightness of 5.65/'blob' - a ratio of 1.38. This is in close agreement with the ratio of the 27keV ^{125}I /20 keV ^{103}Pd photon energies being 1.35.

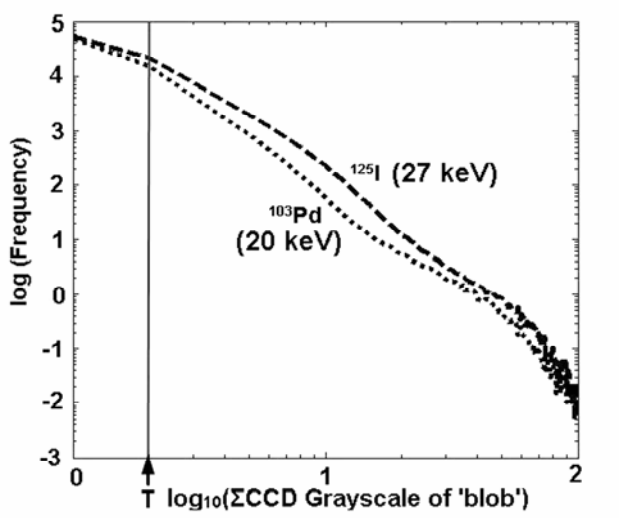

Fig. 5. This linear relationship is consistent with the photon distribution being random. T is the brightness threshold value below which the brightness spots are due to system noise.

B. Imaging Characteristics

Fig. 6 is an image of the seed using the setup described in Fig. 1 plus the polycapillary optic angular filter.

The number of photons counted over the image of the brachytherapy seed was 114,156. The exposure count estimated using (1) with L = 2mm and area of activity 0.7x3.0mm^2 was 289,070 photons over the 500 second acquisition period, i.e., a 39% efficiency of the optic.

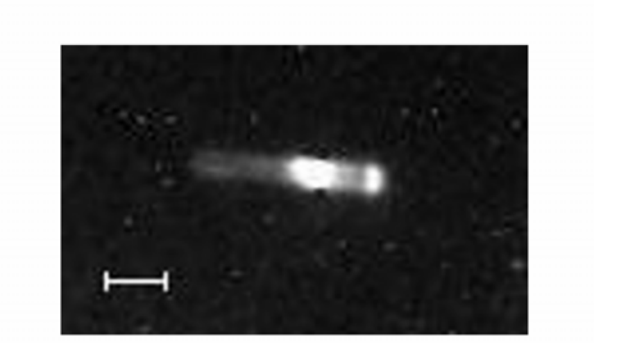

Fig. 6. Image of the ^{125}I brachytherapy seed obtained by summing all the frames over a 500 second period. The photon count over the spheres was 114,156. Scale bar = 1mm.

Fig. 7 is a CT image of the ^{125}I seed generated with another micro-CT scanner.

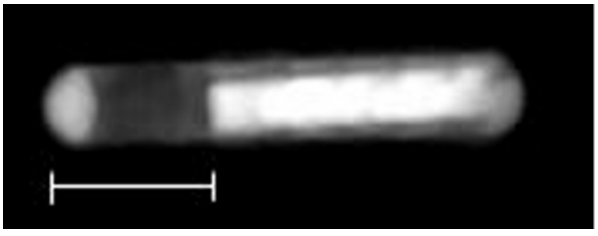

Fig. 7. Maximum intensity projection CT Image of the ^{125}I brachytherapy seed.. . Scale bar = 1mm.

C. Discussion

This approach for x-ray photon counting and energy discrimination imaging, based on an image intensifier and a fast-readout CCD imaging array, is sufficiently efficient and precise to be suitable for micro-CT and some micro-SPECT applications. This approach was inspired by the work in H Barrett's group [5], [6] – the main difference being that they used a coded pin-hole aperture approach for imaging which can not be used for x-ray imaging whereas we used a polycapillary optic which can be used for both x-ray imaging and the nuclide imaging without changing the system (i.e. magnification, distortions, efficiency etc remains identical for the x-ray and radionuclide). Another approach for photon counting and energy discrimination involves use of direct x-ray to electron conversion by use of a CdTe detector array. This does not need an intensifier but its pixel resolution is either of the order of 1mm [7] or 55µm [8].

REFERENCES

[1] The MathWorks™, Inc. Matlab® The Language of Technical Computing, R2008a. http://www.mathworks.com

[2] R. F. Von, "Multiple Fractal Aggregation," *J. Stat. Phys*. vol. 36, pp. 861-872, 1984.

[3] S. M. Jorgensen, M. S. Chmelik, D. R. Eaker, C. A. MacDonald, E. L. Ritman, "A polycapillary x-ray optics-based integrated micro-SPECT/CT scanner," *Proc SPIE - Developments in X-ray Tomography IV*, vol. 5535, pp. 36-42, 2004.

[4] C. A. MacDonald, W. M. Mail, W. M. Gibson, S. M. Jorgensen, E. L. Ritman, "Micro gamma camera optics with high sensitivity and resolution," *Proc SPIE – Med. Imaging 2005: Physics of Med. Imaging*, vol. 5745, pp.1-6, 2005.

[5] B. W. Miller, H. H. Barrett, L. R. Furenlid, H. B. Barber, R. J. Hunter, "Recent advances in BazookaSPECT: real-time data processing and development of a gamma–ray microscope," *Nucl. Instrum. Meth. A*, vol. 59, no. 1, pp. 272-275, 2008.

[6] B. W. Miller, H. B. Barber, H. H. Barrett, D. W. Wilson, L. Chen, "A low-cost approach to high resolution, single-photon, imaging using columnar scintillators and image intensifiers," *Conference Record of 2006 IEEE Nucl. Sci. Symp*., vol. 6, pp. 3540-3545, 2008.

[7] E. C. Frey, K. Taguchi, M. Kapusta, J. Xu, T. Orskaug, I. Ninive, D. Wagenaar, B. Pratt, B.M.W Tsui, "Microcomputed-tomography with a photon-counting X-ray detector," Medical Imaging 2007: Physics of Medical Imaging, *Proc. of SPIE* vol. 6510, pp. 6510R, 2007.

[8] R. Ballabriga, M. Campbell, E.H.M. Heijne, X. Llopart, L. Tlustos, "The Medipix3 Protoype, a pixel readout chip working in single photon counting mode with improved spectrometric performance," *IEEE Trans. Nucl. Sci*., vol. 54, no. 5, pp. 1824-1829, Oct. 2007.